Review Article

OpenSim-Based Coupled Lower Limb Rehabilitation Robots

Wajid Khali*

University of Shanghai for Science and Technology, Shanghai, China

***Corresponding author:** Wajid Khalil Khali, MSs
University of Shanghai for Science and Technology, Shanghai, China
Email: wajidkhalilpt@gmail.com

ORCID ID
Wajid Khali: 0009-0001-9550-8928

Article info:
Received: 23 Nov 2025
Accepted: 14 Dec 2025

Citation: Wajid K. OpenSim-Based Coupled Lower Limb Rehabilitation Robots. Journal of Modern Rehabilitation. 2026;20(4):?-?

Running Title: OpenSim-Based Coupled Lower Limb Rehabilitation Robots

Abstract
This study introduces a human-machine model utilizing OpenSim. It examines the impact of a passive (unactuated) lower-limb rehabilitation exoskeleton on biomechanics during ambulation. The model assesses how well the joints are aligned, how the muscles are used, and how well the design performs. The exoskeleton is made of T6061 aluminum alloy, which makes it light and easy to move. Each leg has three active joints and two passive joints that work in the sagittal plane. Musculoskeletal and exoskeleton models are simulated together in MATLAB and OpenSim. MATLAB scripts set their dynamic properties. A six-degree-of-freedom bushing models the interaction between the human and the exoskeleton at contact points. Joint angles come from experimental gait measurements. A residual-reduction algorithm reduces dynamic errors while keeping the resulting residual forces and moments within acceptable limits. Muscle activations and forces are estimated using computed muscle control, which follows joint paths. Simulations show that even in passive mode, the exoskeleton increases overall lower-limb muscle activation by more than 50% compared to walking without assistance. Significant increases occur in the rectus femoris, gluteus maximus, semimembranosus, and vastus lateralis. Joint torques also change: swing-leg hip and knee torques decrease by about 50%, support-leg torques increase because of the load, and ankle torque adjusts for compensation. These non-invasive simulations show reduced torque variability and support better design updates. This leads to improved exoskeleton alignment and evaluation before physical prototyping.
Keywords: Exoskeleton device; Musculoskeletal system, gait; Biomechanical phenomena; Muscle activation; Joint torque; Simulation models; Passive assistance

1.Introduction

The human musculoskeletal simulation system plays a crucial role in supporting motor disabilities and hemiplegia by assisting in the development of rehabilitation robots. Safety, comfort, and biomechanical evaluation are key factors in this process. Some challenges include the system's complex degrees of freedom, inadequate real-time connection between exoskeletons and joints, slow research and development timelines, and a lack of rehabilitation metrics. To tackle these issues, this research uses the OpenSim API for a human-machine coupling model. It examines muscle energy recruitment and biomechanical changes during rehabilitation. The study examines sagittal-plane movement and the coordination of muscle function. This is important for controlling how people walk and making exoskeletons. The study investigates muscle force, muscle activation, and joint torque by simulating ambulation with and without a passive lower-limb exoskeleton. This lays the groundwork for better exoskeletons and better-designed robot rehabilitation systems.

Computer-assisted modeling allows us to assess the interaction forces between exoskeletons and the human skeleton during prototype development. However, the dynamic redundancy of the musculoskeletal system makes it difficult to model human-robot contact and movement accurately. Previous studies have used OpenSim around the world to explore different exoskeleton-human interactions. Domestic research has focused on OpenSim modeling theory and procedures. For example, Li Linjie et al. developed a lower limb musculoskeletal model using OpenSim-based biomechanical simulation. They applied dynamic optimization to analyze Achilles tendon load and muscle-tendon elongation. Zhou constructed a human-machine coupling model for both walking and running, using muscle calculation tools to evaluate changes in muscle force, energy metabolism, and the effects of lower-limb exoskeletons.

This research builds on prior studies by presenting a modular lower-limb rehabilitation exoskeleton. The coupling model connects the wearable device to the human musculoskeletal system using MATLAB and OpenSim. It examines muscle force, activation, and joint torque before and after exoskeleton use to better understand how humans and machines work together biomechanically. The study shows that a coupling model based on OpenSim will help people understand how much torque is needed at joints. This is good advice for making leg exoskeletons.

2.Design of Lower Limb Rehabilitation Exoskeleton Model

To meet portability and wearability goals, the robot's main support rods and telescopic modules were made from Aluminum alloy T6061. This material is tough, light, and rust-resistant. The kinematic structure of the exoskeleton puts the joint axes as close as possible to the anatomical axes of the knee, hip, and ankle. This makes it less likely that things will get out of line during the move. We determined the mass, center of mass, and inertia of each exoskeleton link and entered them into MATLAB to run a precise dynamic simulation. Figure 1 illustrates a simplified model of the exoskeleton, highlighting the key design elements.

Fig. 1: Lower limb rehabilitation exoskeleton model.

3.Human-Machine Coupling Model Construction

In the joint simulation environment of MATLAB and OpenSim API, we create a human-exoskeleton coupling model. MATLAB sets up a connection to the OpenSim library for data exchange. The physical properties of the exoskeleton components, including mass, center of mass, and inertia, are defined in MATLAB scripts. The OpenSim human musculoskeletal model is imported into MATLAB. We then assemble each part of the exoskeleton into the human skeletal model using joints that replicate human movements. To simulate forces and torques, we add spring-damping components at each contact point between the human and the machine.

Each leg has three active degrees of freedom: hip flexion-extension, knee flexion-extension, and ankle plantarflexion-dorsiflexion. It also includes two passive joints: hip rotation and ankle adduction-abduction, which allow for twisting and side-to-side movements. For the simulation, we limit sagittal-plane movements to study flexion-extension and the timing of muscle activation. The spring-damping elements, or bushing force components, provide three rotational and three translational degrees of freedom, making a total of six at each contact point. These connect the exoskeleton parts to the human body, enabling realistic force transmission. Figure 2 shows the coupled model and bushing force points.

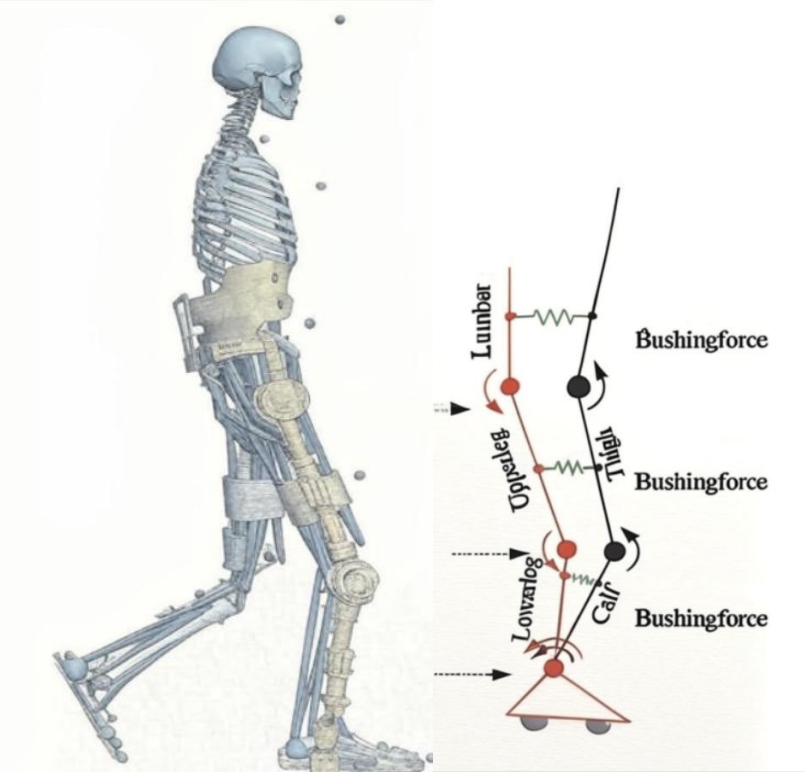

Fig. 2: Human-Exoskeleton Coupling Model.

During OpenSim simulation of the exoskeleton model in Figure 1 The kinematic calibration scaling is complete. The OpenSim API changes the musculoskeletal model to fit the person's body size. Then we solve for the inverse kinematics and check them against motion capture data to ensure they are right. The Residual Reduction Algorithm (RRA) reduces the likelihood of errors when computing forward dynamics.

We measure the accuracy of the RRA output with maximum (Max) and root-mean-square (RMS) residuals, as shown in Table 1 and Figure 3. These values indicate that the residual forces and moments fall within the Effective and Sufficient ranges. This shows that the coupled model is helpful for simulating muscle force and joint torque.

Table. 1: Threshold evaluation range of human-machine coupling model RRA results.

Threshold	Effective	Sufficient	Deficient
MAX Residual Force(N)	0-10N	10-20N	>25N
RMS Residual Force(N)	0-5N	5-10N	>10N
MAX Residual Moment (Nm)	0-50Nm	50-75Nm	>75Nm
RMS Residual Moment (Nm)	0-30Nm	30-50Nm	>50Nm
MAX PErr (trans, cm)	0-2cm	2-5cm	>5cm
RMS PErr (trans, cm)	0-2cm	2-4cm	>4cm
MAX PErr (rot, deg)	0-2deg	2-5deg	>5deg
RMS PErr (rot, deg)	0-2deg	2-5deg	>5deg

PErr: Position Error

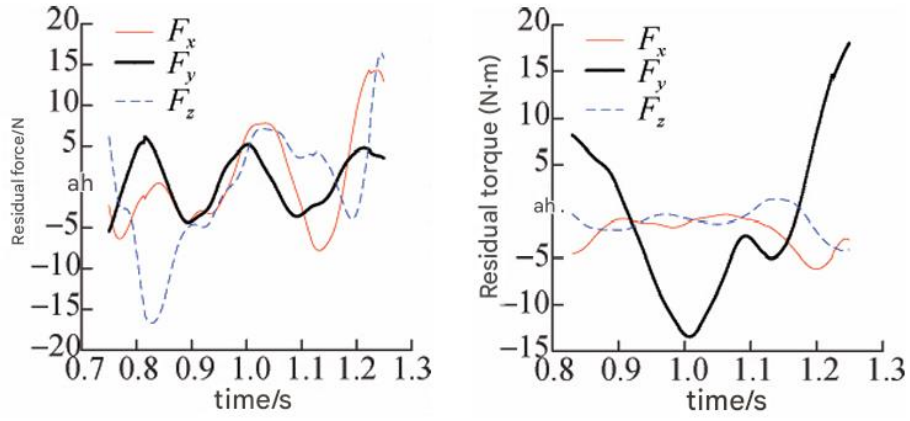

(a) Remaining capacity (b) Residual torque

Fig. 3: Time-varying curves of residual force (Fy) and residual moment (My) in the human-machine coupling model, which prove that the values do not go beyond reasonable limits.

4. Investigation into Alterations in Lower Limb Muscle Properties

4.1 Kinematic Simulation of Human Lower Limb Motion

After minimizing the influence of residual forces and residual torque (unwanted extra forces and rotating effects) on kinematic computations, the human-machine coupling model is reprocessed using OpenSim-based muscle control (Computed Muscle Control (CMC), Computed Muscle Control: an algorithm to estimate muscle effort) to determine variations in muscle strength and energy expenditure during walking with a wearable exoskeleton**.** This process recalculates muscle activation levels and introduces closed-loop control (a system that continuously makes corrections) of activations to provide accurate joint-angle tracking based on the RRA algorithm's output.

The muscle force generated by the human body at each instance is primarily affected by three factors: activation value (A), normalized muscle length (L), and normalized muscle contraction velocity (V)**.** Changes in joint torque within the musculoskeletal model not only indicate the operational state of the human-machine coupling model but also reflect the rhythmic contractions of muscles coordinating skeletal movement around the joints.

As illustrated in Figure 4, the hip and knee joint torque of the right supporting leg is influenced by the exoskeleton’s external gravitational forces, resulting in increased activation of the flexor and extensor groups of muscles, paralleled by a concomitant increase in joint torque. The left swing leg is passive mainly within the limits set by the exoskeleton. Each hip and knee joint torque output, compared with baseline walking without an exoskeleton, shows a decrease in required biological torque of approximately 50%, with ankle joint torque showing slight increases.

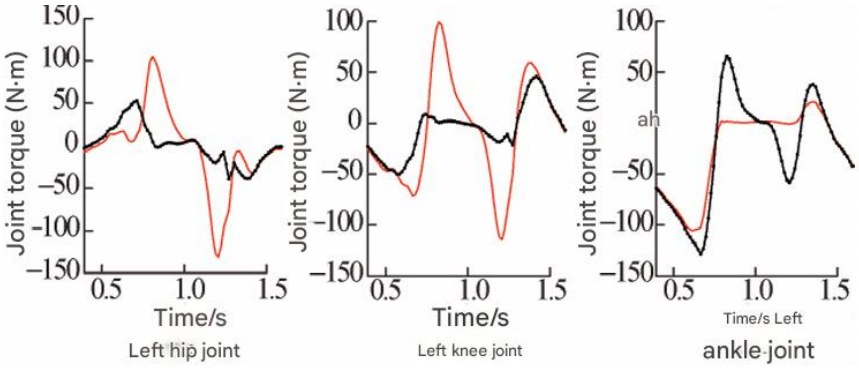

Fig. 4: Joint torque variation curve in the coupling model.

4.2 Study on Muscle Activity Characteristics of the Coupled Model

Variations in muscle activation provide insights into changes in lower-limb muscle strength during exoskeleton use. Muscle strength at any instant is governed by activation value, normalized muscle length, and normalized contraction velocity.

This study focuses on:

- Three single-joint muscles on the front of the right leg: Psoas Major, Vastus Lateralis, and Tibialis Anterior**.**
- Three double-joint muscles: Rectus Femoris, Vastus Lateralis, and Medial Head of Gastrocnemius**.**
- Three single-joint muscles on the back of the leg: Gluteus Maximus, Biceps Femoris (short head), and Soleus**.**

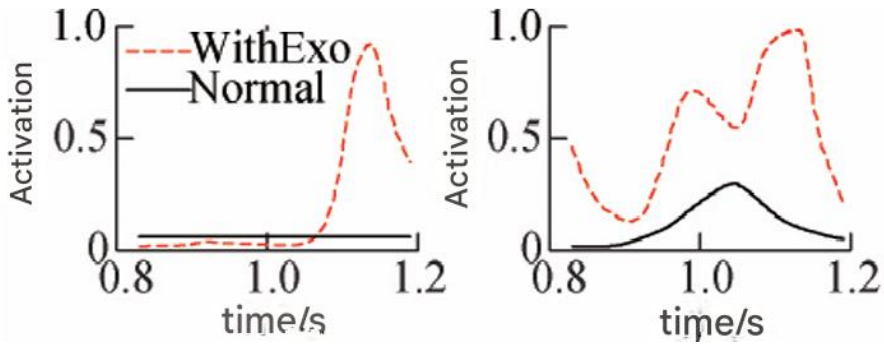

Gluteus Maximus **Rectus Femoris**

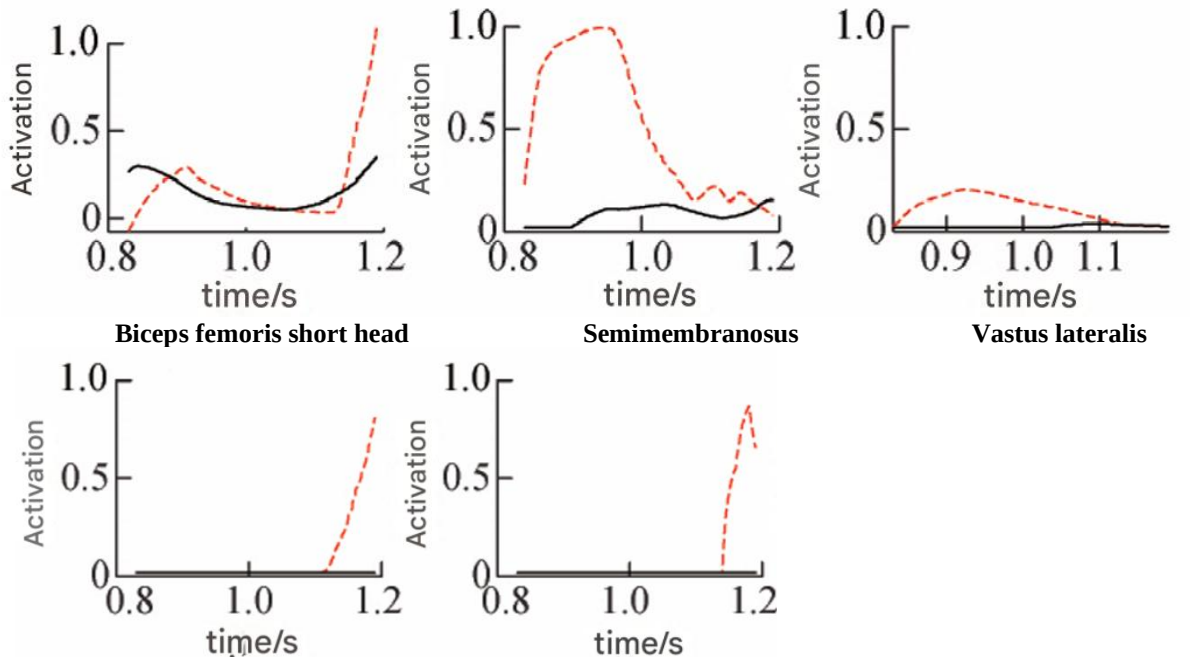

Fig 5: Right thigh muscle activation curve.

During the initial phase of OpenSim-based muscle control, the two knee extensors (Vastus Lateralis and Rectus Femoris) contract to produce extension force, facilitating knee extension and maintaining lower limb stability. At mid- to late-gait cycle, the Rectus Femoris elevates its level of activation by over 50% above baseline walking without an exoskeleton when subjected to external resistance, in conjunction with the Vastus Lateralis to stabilize the knee.

The Vastus Lateralis force curve in Figure 6 shows the contribution of these knee extensors during motion.

Supporting muscles: the Biceps Femoris (short head) and Semimembranosus engage during the early stage of knee extension. The contraction of the Semimembranosus increases with hip extension, facilitating the rate of force production. Toward the end of the cycle, the muscles contribute to flexing the knee at a higher rate of force recruitment than during baseline walking.

The Rectus Femoris and Semimembranosus remain active throughout the movement.

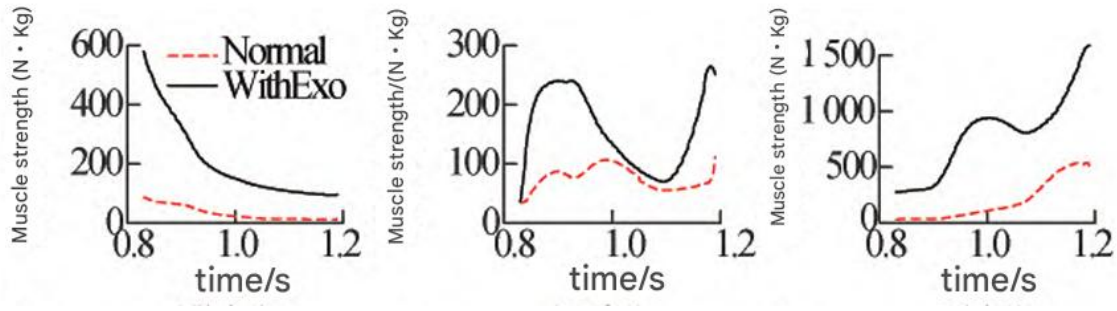

Gluteus Maximus Rectus Femoris Psoas Major

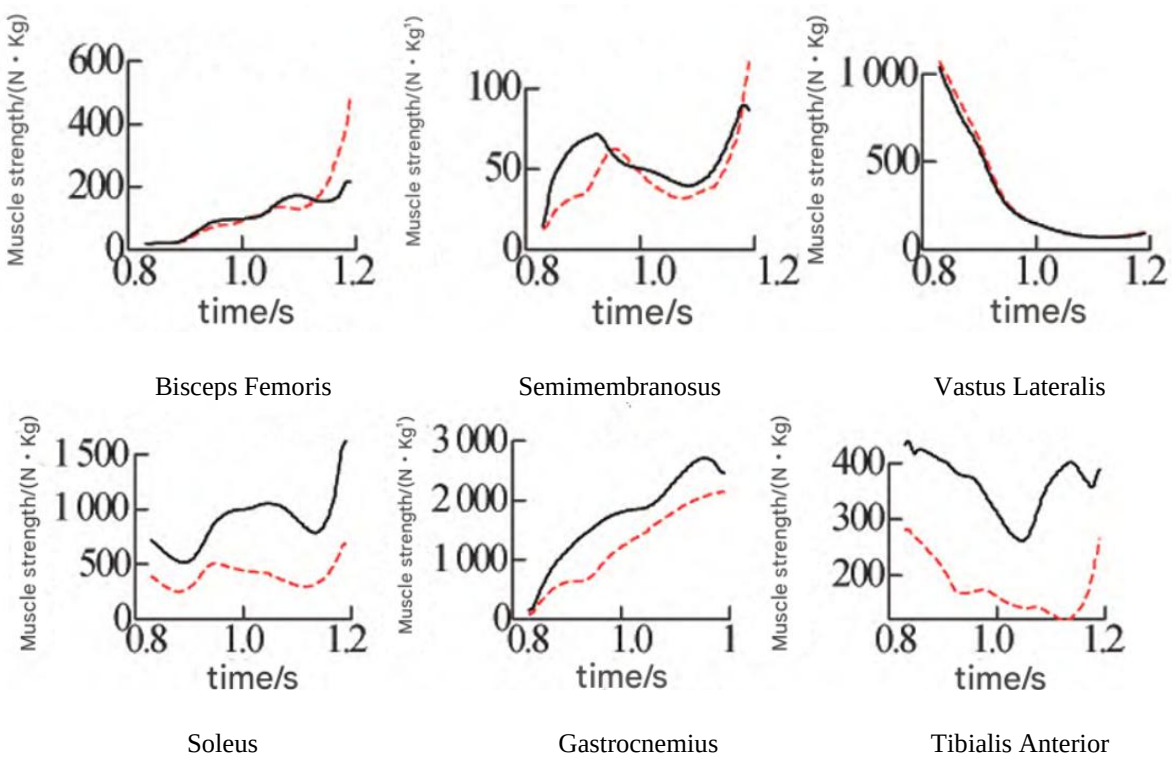

Fig. 6: Right thigh muscle strength curve.

Analysis of Figure 5 and 6 shows that the overall muscle strength of the human-machine coupling model varies under the influence of the exoskeleton, but the overall trend of the right supporting leg is similar to normal walking. Because the exoskeleton restricts abduction, adduction, and rotation of the hip joint, muscles including Gluteus Maximus, Rectus Femoris, Psoas Major, and Semimembranosus are most affected. In the late gait cycle, although the Medial Head of the Gastrocnemius no longer generates ankle plantarflexion torque, it remains active to support knee flexion and stabilize the center of gravity.

According to OpenSim-based simulations, the net muscle force is greatly augmented during exoskeleton wear, even without active assistance. Compared to direct musculoskeletal simulations without exoskeleton interaction, the human-machine coupling model provides a more accurate characterization of the muscle requirements using wearable exoskeletons and proposes avenues for iterative design optimization.

5. Results

Simulation results from the human-machine coupling model developed in OpenSim and MATLAB demonstrated a significantly better musculoskeletal response with an exoskeleton on the lower extremities, even without actuating the joints.

The average activation of the main lower limb muscle groups rose significantly. This increase in muscle force closely matched the level of muscle activity, leading to total muscle strength gains over 50% compared to the baseline. In passive mode, torque production at the swing leg joints, which are the hip and knee, dropped by about 50%. Meanwhile, the ankle joints showed a slight

increase in torque, indicating a compensation mechanism during walking. The hip and knee joint torque of the right supporting leg displayed a clear upward trend, mainly due to the exoskeleton's gravitational load. This was linked to rhythmic contractions of the flexor and extensor muscles that produced immediate muscle force to help maintain balance throughout the gait cycle.

The intricate patterns of muscle activation demonstrated a greater than 50% increase in rectus femoris activation during the mid-to-late gait cycle, enhancing knee stability. Alternating patterns of activation were also observed in the vastus lateralis, short head of the biceps femoris, and semimembranosus, which functioned together in a coordinated fashion to aid in knee flexion and hip extension. The medial head of the gastrocnemius had maintained high levels of activity during the late phase of gait, causing knee flexion and stabilization of the body's center of gravity in spite of the elimination of ankle plantarflexion torque.

To thoroughly assess the accuracy and stability of the simulation, the Residual Reduction Algorithm (RRA) was used to reduce dynamic inconsistencies in the forward dynamic simulations. This follows the established OpenSim modeling protocols. The evaluation metrics, specifically the magnitudes of residual forces and moments, consistently stayed within the 'GOOD' threshold set by the OpenSim Best Practices Guidelines (root mean square residual forces < 5% body weight and moments < 1 Nm/kg). This agreement with accepted biomechanical modeling standards shows that the human and machine coupling model has reliable dynamic performance during steady-state walking.

6. Discussion

This study highlights the importance of the OpenSim-based human-machine coupling model as a key tool for improving lower-limb rehabilitation exoskeleton development. The model allows for detailed analysis of muscle use, joint torque, and interactions between humans and exoskeletons. This helps in systematically evaluating functional outcomes and design features before creating physical prototypes. In addition, the model's ability to predict outcomes provides valuable insights into refining exoskeleton mechanics. It supports data-driven design changes and offers a practical way to evaluate possible therapeutic effects and safety. Ultimately, using this integrated simulation framework strengthens the thoroughness of preclinical assessments for exoskeletons and guides the transition of assistive technologies from simulations to real-world clinical use.

The findings showed that core muscle force output nearly doubled. At the same time, torque variations in passive mode decreased by about 50%. This confirms the model's potential to improve rehabilitation outcomes.

The escalation of muscle activation observed in this study is consistent with the pattern of increased force, suggesting that the exoskeleton's mass inertia and joint configuration further compel muscle recruitment. These effects have only been partially modelled as conventional body loads and highlight the advantage of a human-machine coupling approach to biomechanics.

Nevertheless, this study does have limitations. Each analysis focuses on the sagittal plane, which precludes multi-planar movement patterns and may reveal increased muscle assistance due to neglected dynamics. Moreover, there is no experimental validation, which limits the ability to generalize simulation findings. Notably, there is a contrast with prior studies reporting exoskeleton assistance through active torque generation, as the passive assistance mode adopted in this model emphasizes torque reduction rather than generation. Thus, this model offers a new way to think about biomechanical influence, yet it limits its scope to less than prior studies.

Though other authors reported similar patterns of variation in muscle force, their inclusion of different locomotor conditions (e.g., walking and running) suggests that the current model does

not account for multi-plane interactions or individual variability in the gait. Rhythmic torque increases at the hip and knee joints likely represent coordinated flexor-extensor activity, and the increases in torque at the ankle joints may represent compensatory behavior unique to each subject. Future validation using electromyography (EMG) and motion capture data will take place to establish simulated muscle activations compared to experimental gold standards. Upcoming work will focus on trials with humans to confirm simulation results, further developing the controller for multi-plane motion, and incorporating energy-efficient materials and adjustable features based on the research of Veneman et al. (2007) for gait rehabilitation and biomechanical improvement.

7. Conclusion

This study investigated the long-term biomechanical implications of exoskeleton systems and addressed the challenges of directly analyzing their effects on the human musculoskeletal system. Using a combined OpenSim–MATLAB modeling framework, the research examined physiological responses during unassisted and exoskeleton-assisted walking, with emphasis on the effects on muscle activation, metabolism, and force generation.

The findings show that mass inertia and joint constraints imposed by the exoskeleton significantly increased mean activation of major muscle groups and whole-muscle strength. This coupling of human and machine provides a solid theoretical foundation for optimizing the functional and structural design of exoskeletons for lower extremity rehabilitation.

Nonetheless, relying on simulation instead of human experimentation is a major limitation. Future research will broaden the model to include real human trials. It will also extend MATLAB, OpenSim simulations to assess the biomechanical effects of human-machine interaction in various rehabilitation scenarios. Additionally, further optimization of the exoskeleton's control system will be pursued to enhance adaptability, reduce metabolic cost, and improve therapeutic effectiveness.

Funding:
This research received no external funding

Acknowledgements:
Not applicable

Authors' contributions:
The author is the sole contributor to this work

Conflict of interest:
None

References:

1. Banala SK, Kim SH, Agrawal SK, Scholz JP. Robot-assisted gait training with active leg exoskeleton (ALEX). *IEEE Trans Neural Syst Rehabil Eng.* 2008;17(1):2–8. doi:10.1109/TNSRE.2008.2008282.
2. Bortoletto R, Sartori M, He F, Pagello E. Modeling and simulating compliant movements in a musculoskeletal bipedal robot. In: Proceedings of the International Conference on Simulation, Modeling, and Programming for Autonomous Robots; 2012 Nov 5-8; Tsukuba, Japan.

3. Dollar AM, Herr H. Lower extremity exoskeletons and active orthoses: challenges and state-of-the-art. *IEEE Trans Robot.* 2008;24(1):144-158. doi:10.1109/TRO.2007.914781.
4. Donati M, Vitiello N, De Rossi SMM, et al. A flexible sensor technology for the distributed measurement of interaction pressure. *Sensors (Basel).* 2013;13(1):1021-1045. doi:10.3390/s130101021.
5. Ferrati F, Bortoletto R, Pagello E. Virtual modelling of a real exoskeleton constrained to a human musculoskeletal model. In: Proceedings of the Conference on Biomimetic and Biohybrid Systems; 2013 Jul 29-Aug 1; London, UK.
6. Grey JE, Enoch S, Harding KG. ABC of wound healing: venous and arterial leg ulcers. *BMJ.* 2006;332(Suppl S4). doi:10.1136/bmj.332.7537.S2.
7. Kawamoto H, Hayashi T, Sakurai T, Eguchi K, Sankai Y. Development of a single leg version of HAL for hemiplegia. In: 2009 Annual International Conference of the IEEE Engineering in Medicine and Biology Society; 2009 Sept 3-6; Minneapolis, MN.
8. Li LJ, Zhang YX. Biomechanical simulation of Achilles tendon strains during hurdling. *Adv Mater Res.* 2013;647:462-465. doi:10.4028
9. Manns P, Sreenivasa M, Millard M, Mombaur K. Motion optimization and parameter identification for a human and lower back exoskeleton model. *IEEE Robot Autom Lett.* 2017;2(3):1564-1570. doi:10.1109/LRA.2017.2678567.
10. Reinbolt JA, Seth A, Delp SL. Simulation of human movement: applications using OpenSim. *Procedia IUTAM.* 2011;2:186-198. doi:10.1016/j.piutam.2011.04.018.
11. Rodríguez-Fernández A, Lobo-Prat J, Font-Llagunes JM. Systematic review on wearable lower-limb exoskeletons for gait training in neuromuscular impairments. *J Neuroeng Rehabil.* 2021;18(1):22. doi:10.1186/s12984-021-00813-2.
12. Strausser KA, Kazerooni H. The development and testing of a human-machine interface for a mobile medical exoskeleton. In: 2011 IEEE/RSJ International Conference on Intelligent Robots and Systems; 2011 Sept 25-30; San Francisco, CA.
13. Uchida TK, Hicks JL, Dembia CL, Delp SL. Stretching your energetic budget: how tendon compliance affects the metabolic cost of running. *PLoS One.* 2016;11(3):e0150378. doi:10.1371/journal.pone.0150378.
14. Vallery H, Van Asseldonk EH, Buss M, Van Der Kooij H. Reference trajectory generation for rehabilitation robots: complementary limb motion estimation. *IEEE Trans Neural Syst Rehabil Eng.* 2008;17(1):23–30. doi:10.1109/TNSRE.2008.2008280.
15. Veneman JF, Kruidhof R, Hekman EE, et al. Design and evaluation of the LOPES exoskeleton robot for interactive gait rehabilitation. *IEEE Trans Neural Syst Rehabil Eng.* 2007;15(3):379–386. doi:10.1109/TNSRE.2007.903919.
16. Zhang J, Fiers P, Witte KA, et al. Human-in-the-loop optimization of exoskeleton assistance during walking. *Science.* 2017;356(6344):1280-1284. doi:10.1126/science.aah7654.
17. Zhao C, Liu Z, Ou Y, Zhu L. Mechanical structure design and motion simulation analysis of a lower limb exoskeleton rehabilitation robot based on human-machine integration. *Sensors (Basel).* 2025;25(5):1611. doi:10.3390/s25051611.
18. Su D, Hu H, Wu X, Shang J, Luo H. Review of adaptive control for stroke lower-limb exoskeleton rehabilitation robots based on motion-intention recognition. *Front Neurorobotics.* 2023;17:1186175. doi:10.3389/fnbot. 2023.1186175.
19. Zhang Y, Zhao W, Wan C, et al. Exoskeleton rehabilitation robot training for balance and lower limb function in sub-acute stroke patients: a pilot, randomized controlled trial. *J Neuroeng Rehabil.* 2024;21:98. doi:10.1186/s12984-024-01391-0.

20. Zhu Z. Design and motion control of exoskeleton robot for lower limb rehabilitation. *Frontiers in Neuroscience.* 2024;18:1355052. doi:10.3389/fnins.2024.1355052.